THE JOURNAL OF PHYSICAL CHEMISTRY A LETTERS

2008, *112,* 10708–10712
Published on Web 09/11/2008

Adsorption and Structure of Water on Kaolinite Surfaces: Possible Insight into Ice Nucleation from Grand Canonical Monte Carlo Calculations

T. Croteau, A. K. Bertram, and G. N. Patey*

Department of Chemistry, University of British Columbia, Vancouver, British Columbia, Canada V6T 1Z1

Received: June 25, 2008; Revised Manuscript Received: August 03, 2008

Grand canonical Monte Carlo calculations are used to determine water adsorption and structure on defect-free kaolinite surfaces as a function of relative humidity at 235 K. This information is then used to gain insight into ice nucleation on kaolinite surfaces. Results for both the SPC/E and TIP5P-E water models are compared and demonstrate that the Al-surface [(001) plane] and both protonated and unprotonated edges [(100) plane] strongly adsorb at atmospherically relevant relative humidities. Adsorption on the Al-surface exhibits properties of a first-order process with evidence of collective behavior, whereas adsorption on the edges is essentially continuous and appears dominated by strong water lattice interactions. For the protonated and unprotonated edges no structure that matches hexagonal ice is observed. For the Al-surface some of the water molecules formed hexagonal rings. However, the a_o lattice parameter for these rings is significantly different from the corresponding constant for hexagonal ice (*Ih*). A misfit strain of 14.0% is calculated between the hexagonal pattern of water adsorbed on the Al-surface and the basal plane of ice *Ih*. Hence, the ring structures that form on the Al-surface are not expected to be good building-blocks for ice nucleation due to the large misfit strain.

I. Introduction

Ice clouds play an important role in the Earth's radiation budget by reflecting and absorbing solar and terrestrial radiation.[1] Ice particles, and hence ice clouds, form when ice nucleates on or in aerosol particles present in the atmosphere. This can occur either homogeneously (in a liquid aerosol particle) or heterogeneously (on the surface of a solid aerosol particle such as mineral dust or soot). Heterogeneous ice nucleation has been studied for many years, yet it remains poorly understood, especially on a molecular level.[2]

Mineral dust particles, which are abundant in the atmosphere, are thought to play an important role in ice cloud formation in the atmosphere.[3] Common minerals found in aerosolized dust include quartz, illite, muscovite, chlorite, kaolinite, and calcite.[4] In the following we will focus on kaolinite particles which make up between 5−10% of the aerosolized mass of mineral dust.[4] In addition, kaolinite is known to be an especially effective ice nucleus on the basis of laboratory studies.[5] Kaolinite is a type of clay particle and information determined on kaolinite may also lead to a better understanding of other clays.

Kaolinite particles are composed of different surface types, two basal (001) planes and several possible "edges" (other planes). The basal (001) planes in kaolinite are referred to as the Al-surface and Si-surface. The Si-surface is known to be hydrophobic, and the Al-surface, which is terminated by hydroxyl groups, attracts water.[6] Similarly, the edges of kaolinite are terminated by oxygen atoms or hydroxyl groups that can easily be protonated or deprotonated depending on pH.[7] The edges used here are termed protonated and unprotonated edges and are surfaces parallel to the (100) plane. These are hydrophilic surfaces that may play a role in ice nucleation or at least in water adsorption.

The reason kaolinite is a good ice nucleus remains unclear. In has been speculated that the good ice nucleation ability of kaolinite is related to the good crystallographic match between kaolinite surfaces and hexagonal ice surfaces. This implies that kaolinite surfaces have sites that arrange the water molecules in a structure that has similar lattice constants to hexagonal ice. The absorbed water structures may then be good templates for ice embryo formation, because the resulting embryos may have minimal strain due to the good match between the adsorbed water at the kaolinite surface and hexagonal ice.

To quantify the crystallographic match between kaolinite and hexagonal ice, Pruppacher and Klett[2] calculated an apparent crystallographic misfit or disregistry using

$$\delta \equiv \frac{na_{o,N} - ma_{o,i}}{ma_{o,i}}$$

where $a_{o,N}$ is the crystallographic lattice parameter of a particular face of the nucleus, $a_{o,i}$ is the corresponding constant in the ice lattice and n, m are integers chosen such that δ is minimal. Pruppacher and Klett found a good match ($\delta = 1.1\%$) between the basal face of hexagonal ice and the Al-surface of kaolinite if n and m are 3 and 2, respectively. These calculations employed a hypothetical "pseudohexagonal" surface with an a_o lattice parameter of 2.98 to represent the Al-surface, and an a_o lattice parameter of 4.52 for hexagonal ice.

In the present study we investigate the adsorption and structure of water on kaolinite surfaces at 235 K, a temperature relevant for ice nucleation in the atmosphere. Calculations are carried out for four different surfaces, the Al-surface, the Si-surface and protonated and unprotonated edges. The information obtained is used to gain insight into ice nucleation on kaolinite.

10.1021/jp805615q CCC: $40.75

Key questions we address are the following: (1) Does water adsorb on defect-free kaolinite surfaces at 235 K and under typical atmospheric relative humidities? (2) Do the kaolinite surfaces promote adsorbed water molecules to adopt a structure similar to hexagonal ice? If so, these water structures could serve as good building blocks for ice embryo formation because they would impose minimal strain.

Recently, Hu and Michaelides[8,9] used DFT calculations to examine the structure of water on the Al-surface of kaolinite, and the possible implications for ice nucleation. We compare with these previous calculations. Several other groups have also looked at water adsorption on different surfaces in the context of ice nucleation. These calculations are briefly discussed as well.

II. Model and method

In the present calculations, we consider two different water models, the extended single point charge SPC/E[10] and TIP5P-E.[11] Kaolinite is described with the clay force field (CLAYFF) recently developed by Cygan et al.[12] SPC/E is a rigid water model with point charges located at the three atomic nuclei, and all are embedded in a Lennard-Jones (LJ) sphere. This model has been widely used in the past and is known to give accurate results in the liquid state. However, it was found[13] that the SPC/E model does not accurately predict the melting point of ice. In comparison, the TIP5P model of Mahoney and Jorgensen[14] gives a value of 274 K for the melting point. Therefore, the TIP5P-E[11] model, which is a recent reparametrization of the original TIP5P[14] model to account properly for long-range interactions, is also used. In this model, equal positive and negative partial charges are placed at the center of both hydrogen nuclei and at oxygen "lone pairs" locations, respectively, and are embedded in a LJ sphere centered at the oxygen nucleus. The use of two different water models is useful as it gives an indication of the sensitivity of our results to the water model employed.

CLAYFF is an atomistic model again constructed of LJ spheres and point charges. In its general form the CLAYFF model can be flexible, but for practical purposes we employ a rigid lattice set in the stable kaolinite structure as obtained by Bish.[15] The total interaction energy for our model is given by the sum of Coulombic and van der Waals terms

$$U = \frac{1}{4\pi\varepsilon_o}\sum_{i\neq j}\frac{q_i q_j}{r_{ij}} + \sum_{i\neq j} D_{o,ij}\left[\left(\frac{R_{o,ij}}{r_{ij}}\right)^{12} - 2\left(\frac{R_{o,ij}}{r_{ij}}\right)^{6}\right] \quad (1)$$

where q_i is the charge on site i, ε_o is the permittivity of free space, and we have used the notation of ref 12. The summations are over all interaction sites in the system including water molecules and the kaolinite lattice. All short-range interactions in the van der Waals term are represented by the LJ potential. The parameters involved in the kaolinite-water interactions are given in ref 12.

The simulation cell employed (Figure 1) is similar to that used in earlier work involving two slabs and long-range electrostatic interactions.[16,17] The basic cell contains one of the four surfaces displayed in Figure 2 and is repeated periodically in the x and y dimensions. The (x, y) cell dimensions are (30.921 Å, 35.7676 Å) for the Al- and Si-surfaces, and (29.524 Å, 35.7676 Å) for the edges. These "single-layer" slabs consist of 816 atoms (sites) that correspond to the translation of 48 kaolinite unit cells obtained from the ideal formula $Al_2Si_2O_5(OH)_4$.

The short-range interactions were calculated by employing a spherical cutoff of half the box length, and the total Coulombic energy was obtained using the usual three-dimensional Ewald method.[16−18] An empty space (Figure 1) of 107 Å was found to be sufficient to avoid unphysical interactions with images in the z direction.

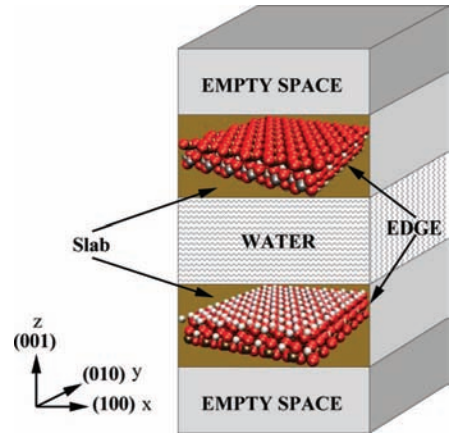

Figure 1. Sketch of the simulation cell.

Most simulations were performed with the two slabs separated by 30 Å. Some were performed at a separation of 60 Å to verify that water adsorption at one surface is not significantly influenced by the presence of the other. Thus, before the "filling transition" at saturation (corresponding to bulk condensation of the vapor) the system behaves as two surfaces adsorbing independently, and results for both surfaces can be averaged to improve the statistics. Calculations were also performed with thicker kaolinite slabs, and adding an extra layer was shown to have no significant effect on water adsorption.

Edge configurations (Figure 2c,d) were constructed by cleaving the Al-surface (Figure 2a) parallel to the (100) plane and replicating in the xy plane. The configuration thus obtained represents one limiting case with pH above the isoelectric point (IEP) such that the surface is completely deprotonated.[7] At the other extreme, well below the IEP, all of the surface oxygens would be protonated such that the surface is positively charged. The protonation state of the edges under atmospheric conditions is not known and is likely variable; therefore, we examine both extremes. We find in fact that the water adsorption ability of an edge is not particularly sensitive to the protonation state and is similar for both limiting cases considered (see Figure 3). The protonated edge is modeled by placing protons (with partial charges appropriate to hydroxyl groups)[12] directly above every "bare" oxygen atom with an internuclear distance of 1 Å. To recover global neutrality in our sample, the extra positive charges are countered by distributing an equal negative charge over all of the atoms below the top Al−Si layer. This amounts to adding a small charge (−0.05 e, e is an elementary charge) to each of the 544 atoms below the surface. Again, changing the slab thickness (i.e., reducing the negative charge added per subsurface atom) had no significant effect on the results.

All results reported were obtained employing grand canonical Monte Carlo (MC) calculations.[18] In this method the thermodynamic state is fixed by specifying the volume, V, the temperature, T, and the water chemical potential μ. The number of water molecules in the system, N_W, is allowed to fluctuate. A Monte Carlo step consisted of a particle insertion, deletion, translation or rotation. In all simulations, the system was equilibrated for at least 5×10^7 MC steps. Following equilibration, averages were collected for an additional 2×10^8 or more MC steps.

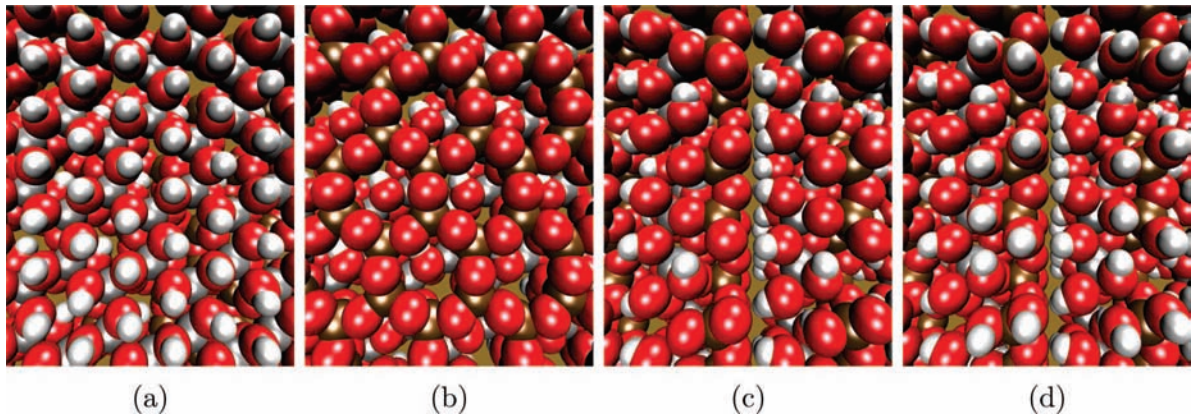

Figure 2. Blown up views of the (a) Al- and (b) Si- surfaces, (c) (100) unprotonated and (d) protonated edges. The oxygen, hydrogen, silicon and aluminum atoms are red, white, brown and gray, respectively.

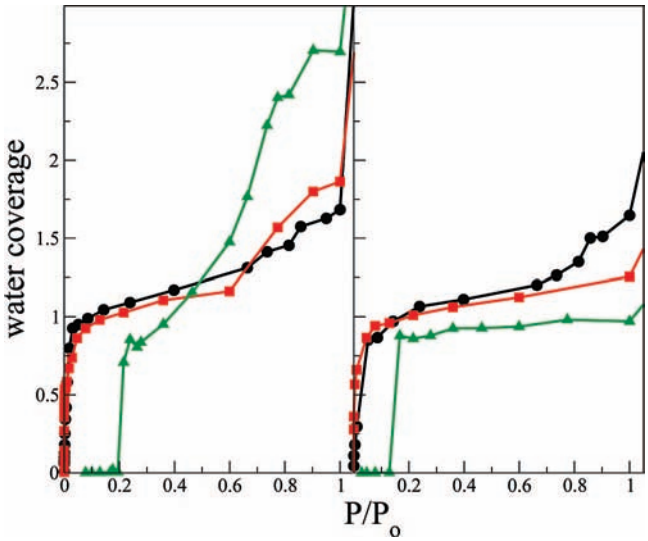

Figure 3. Adsorption isotherms obtained at 235 K using SPC/E (left) and TIP5P-E (right) water models. Results are shown for the unprotonated edge (black circles), protonated edge (red squares), and Al-surface (green triangles).

III. Results and Discussion

Adsorption Isotherms. Adsorption isotherms in the form of the average number of water molecules, $\langle N_W \rangle$, versus the chemical potential, μ, were obtained for all four surfaces. The 235 K adsorption isotherms cast in a more familiar form are plotted in Figure 3. In this plot, the "water coverage" is $\langle N_W \rangle A_W/A$, where A_W is the surface area occupied by a water molecule (taken to be 9 Å^2) and A is the total surface area of the particular face considered ($A = L_x L_y$, where L_x and L_y are the x and y dimensions of the simulation cell). The pressure, P, of the water vapor at equilibrium corresponding to particular chemical potentials was estimated using the ideal gas relationship, $P = e^{\beta\mu}/\beta\Lambda^3$, where $\Lambda = (\beta h^2/2\pi m)^{1/2}$ is the thermal de Broglie wavelength, $\beta = 1/k_B T$, k_B is the Boltzmann constant, and m is the mass of a water molecule. P_0 is the saturated vapor pressure chosen such as to set $P/P_0 = 1$ at the observed filling transition. It is important to remark that the $\langle N_W \rangle$ versus μ isotherms directly obtained in our simulations are accurate and are in no way influenced by the pressure estimates used in the plot. Accurate vapor pressures could in principle be obtained from simulation, but the ideal gas equation is sufficiently accurate to give a qualitative indication of the pressures involved.

For the Si-surface, we found no adsorption before saturation (condensation), and hence no results for this surface are included in Figure 3. This is not surprising because the Si-surface is known to be hydrophobic, and our result is consistent with earlier work.[19] An interesting observation is that both the protonated and unprotonated edges take up water at lower pressures than does the Al-surface, with the protonated edge having the greatest affinity for water. Nevertheless, the relative pressure range, P/P_0, at which adsorption occurs on the Al-surface (Figure 3) is significant for both models, TIP5P-E predicting the largest range. These findings are important because they strongly suggest that edges can contribute significantly to kaolinite's ability to take up water, and perhaps to the heterogeneous chemistry where water is needed for hydrolysis.[20,21]

The results shown in Figure 3 were obtained by increasing the chemical potential from a low value (empty simulation cell) to filling. All surfaces were checked for hysteresis. This was done by starting simulations from a configuration obtained at the last point before filling and decreasing the chemical potential until all water had evaporated. For both edges the curves obtained (not shown) are relatively smooth with little hysteresis. This indicates that the strong surface water interactions are largely responsible for the adsorption, and there is not much suggestion of collective behavior. The situation is different for the Al-surface. Here one notes that the surface coverage (see Figure 3) "jumps" quite quickly from essentially nothing to a monolayer for both SPC/E and TIP5P-E. For the SPC/E at 235 K, this is followed by a second layer and some additional thickening before filling. This behavior was verified by performing simulations with the surface separation increased to 60 Å (not shown). Additionally, for the Al-surface significant hysteresis (not shown) is observed. These observations indicate that collective behavior amongst the water molecules is important for adsorption to occur on the Al-surface. In other words, water condensation onto the Al-surface exhibits features characteristic of first-order processes, whereas condensation onto the edges appears essentially continuous.

A detailed analysis of the water-surface interactions for different surfaces and configurations will be given in a forthcoming article. Here we simply report that the average adsorption energies (in kJ/mol) at 150 K for a single water are (−15.7, −15.6), (−43.1, −41.4), (−69.4, −69.3), (−89.7, −72.0) for the Si-surface, the Al-surface, the unprotonated edge and the protonated edge, respectively, where the first number of each pair is for the SPC/E model and the second number is the TIP5P-E result. We note that the SPC/E and TIP5P-E values are in reasonably good agreement except for the protonated edge where the model discrepancy is significant. Also, it is obvious

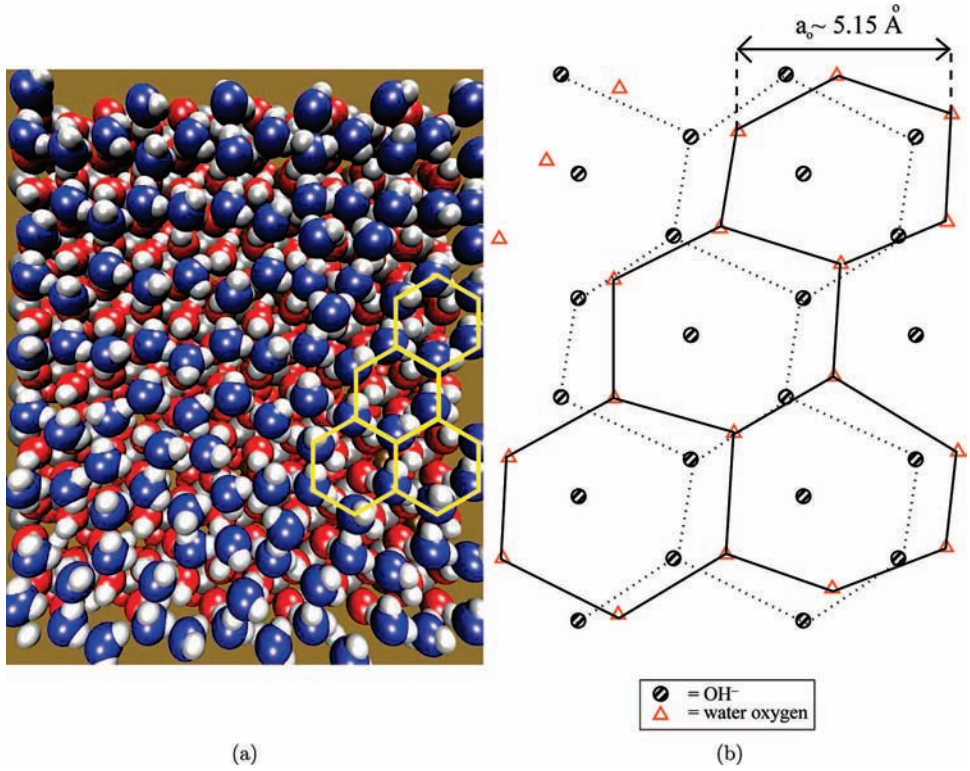

Figure 4. (a) Top view of a monolayer (112 water molecules) on the Al-surface obtained at 235 K with the TIP5P-E model. (b) 2-D projection in the *xy* plane of the yellow hexagonal pattern overlaid in (a) and the underlying hydroxyl groups forming the Al-surface. The a_o lattice parameter of the rings matches that of the lattice (5.1535) but not ice *Ih* (4.52). The water oxygens and hydrogens are blue and white, respectively. The lattice oxygen, hydrogen, silicon and aluminum atoms are red, white, brown and gray, respectively.

that the single molecule binding energies are in accord with the adsorption isotherms discussed above.

Water Structure and Lattice Match. Figure 4a shows a typical monolayer obtained on the Al-surface at 235 K using TIP5P-E. The water molecules are quite uniformly spread, and one can discern loose "networks" with the water molecules clearly interacting with surface atoms and with each other. It is observed that only for the Al-surface can strong correlations amongst the water molecules produce some hexagonal patterns which are easily discernable in Figure 4a. The same patterns are found using SPC/E, but they are more evident for TIP5P-E. Well-defined six-membered ring patterns are not observed on the edges. Instead, on the unprotonated edge, the water molecules primarily interact with the surface in very specific sites along the interlayer junctions (center of Figure 2c) where two kaolinite sheets come into contact and form multiple hydrogen bonds between the basal Al- and Si-surfaces. On the protonated edge, the water molecules prefer to bind first along the hydroxyl hydrogen lines created by protonation (slightly off center in Figure 2d). As more water is adsorbed, a network is created across the surface for both edges.

The hexagonal structure we obtain for kaolinite (Figure 4b) does not match ice *Ih*. The a_o lattice parameter that would be applicable to the hexagonal structures adsorbed on kaolinite is roughly 5.15, significantly different than 4.52, the a_o lattice parameter for hexagonal ice. To estimate the effect of this difference between the a_o lattice parameters, we use the following equation to calculate the strain on the ice embryo due to mismatch[2]

$$\epsilon \equiv \frac{a'_{o,i} - a_{o,i}}{a_{o,i}}$$

where $a_{o,i}$ and $a'_{o,i}$ are the lattice parameters of the ice in the strain-free and strained conditions, respectively. Assuming $a_{o,i} = 4.52$ and $a'_{o,i} = 5.1535$, we obtain a strain of 14.0%. On the basis of Turnbull and Vonnegut,[22] a strain of more than 5% would lead to an additional depression in the nucleation temperature of at least 40 °C, so it is hard to imagine that the hexagonal rings observed in our simulations will be beneficial for ice nucleation due to the possible strain imposed on the ice embryo.

The crystallographic misfit calculations discussed by Pruppacher and Klett[2] (see Introduction) lead to very different conclusions than our GCMC calculations. Their calculations suggest that the actual mismatch between kaolinite and hexagonal ice is only 1.1%, which should result in a very small difference between the a_o lattice parameters of the adsorbed water and hexagonal ice. However, these calculations assume that the water molecules will arrange themselves on the Al-surface with a 3:2 ratio of the a_o lattice parameters. However, the hexagonal structure we obtain for kaolinite (Figure 4b) does not match ice *Ih* but rather fits the roughly hexagonal arrangement of the surface hydroxyl groups on the Al-surface of kaolinite in a 1:1 ratio.

Recently, Hu and Michaelides[8,9] used DFT calculations to study water binding to the Al-surface of kaolinite. They reported that water formed 2-D ice-like layers with a stability matching that of ice *Ih*, but they noted that there was a lattice mismatch between the substrate and ice. They also noted that multilayer ice growth is not favored, being considerably unstable compared to bulk ice. Our calculations, which are applicable to 235 K and relative humidities covering the range important in the atmosphere, are consistent with the picture that emerges from the DFT calculations (presumably 0 K results).

Other previous theoretical studies of ice nucleation on surfaces have shown the possible formation of hexagonal rings. For example, Shevkunov[23,24] studied the structure of water on the surface of a β-AgI crystal as well as in microcracks using a

Monte Carlo approach. In his simulations, the water molecules organized themselves into monolayer islands on a single surface or into multilayered films in a microcrack with clear features of hexagonal ice. Similar patterns were obtained by Taylor and Hale[25] also on a AgI substrate, although they found that the ice-like character did not extend beyond the first water layer. Using molecular dynamics to study different modes of water aggregation on the surface of CaF_2 and BaF_2, Wassermann et al.[26] found that at high coverage an ice *Ih* layer only formed on the BaF_2 substrate and not on the CaF_2 substrate. Hexagonal patterns have also been observed experimentally and studied with DFT calculations for water on metal surfaces.[27,28] Clearly, water structure on a surface is very sensitive to the underlying substrate, which is consistent with the results presented here.

IV. Conclusion

Earlier attempts to understand water adsorption and ice nucleation on kaolinite have focused almost exclusively on the Al- and Si-surfaces. Our calculations demonstrate that edges can also make an important contribution to water uptake, and might well play an important role in heterogeneous surface chemistry that involves water. As expected, the Si-surface is hydrophobic and exhibits no tendency to adsorb water at pressures below saturation. On the Al-surface the adsorption displays first-order characteristics, with evidence of collective behavior provided by the hysteresis observed for adsorption−desorption simulations. Adsorption on the edges is much more continuous, and appears to be dominated by the very strong water-surface interactions.

Despite some differences in adsorption both SPC/E and TIP5P-E give similar monolayer structures. Detailed examination of the structure of the water film on the Al-surface reveals some tendency to form hexagonal patterns, but the observed a_o lattice parameter is significantly different from that of ice *Ih*.

In short we did not observe water structures that closely match the structure of hexagonal ice on any of the surfaces investigated. Hence, our calculations do not confirm previous speculations that kaolinite is a good ice nucleus in part because the crystallographic properties of kaolinite promotes water structures on the surface that closely resemble hexagonal ice. If these structures do form, they are extremely rare and are not the thermodynamically preferred state at the surface. Given this, one may suspect that "active sites" such as cracks, pores, steps, etc., are important for ice nucleation on kaolinite. We are currently investigating this possibility.

Acknowledgment. The financial support of the Natural Science and Engineering Research Council of Canada and the Canadian Foundation for Climate and Atmospheric Science is gratefully acknowledged. This research has been enabled by the use of WestGrid computing resources, which are funded in part by the Canada Foundation for Innovation, Alberta Innovation and Science, BC Advanced Education, and the participating research institutions. WestGrid equipment is provided by IBM, Hewlett-Packard and SGI.

References and Notes

(1) Forster, P.; Ramaswamy, V.; Artaxo, P.; Berntsen, T.; Betts, R.; Fahey, D. W.; Haywood, J.; Lean, J.; Lowe, D. C.; Myhre, G.; Nganga, J.; Prinn, R.; Raga, G.; Schulz, M.; Dorland, R. V. In *Changes in Atmospheric Constituents and in Radiative Forcing., in Climate Change 2007: The Physical Science Basis. Contribution of Working Group I to the Fourth Assessment Report of the Intergovernmental Panel on Climate Change 2007*; Solomon, S., Qin,D., Chen,M., Manning, Z. Marquis, M., Averyt, K. B., Tignor, M., Miller, H. L., Eds.; Cambridge University Press: Cambridge, U.K., and New York, U.S.A., 2007; pp 129−234.

(2) Pruppacher, H. R.; Klett, J. D. *Microphysics of Clouds and Precipitation*, 2nd rev. ed.; Kluwer Academic: Dordrecht, The Netherlands, 1997; pp 329−331.

(3) (a) Cantrell, W.; Heymsfield, A. J *Bull. Am. Meteor. Soc.* **2005**, *86* (6), 795. (b) DeMott, P. J.; Cziczo, D. J.; Prenni, A. J.; Murphy, D. M.; Kreidenweis, S. M.; Thomson, D. S.; Borys, R.; Rogers, D. C. *Proc. Natl. Acad. Sci.* **2003**, *100*, 25–14655.

(4) Glaccum, R. A.; Prospero, J. M. *Mar. Geol* **1980**, *37* (3−4), 295.

(5) Zimmerman, F.; Ebert, M.; Worringen, A.; Sch Weinbruch, S. *Atmos. Environ.* **2007**, *41*, 8219.

(6) Tunega, D.; Gerzabek, M. H.; Lischka, H. *J. Phys. Chem. B* **2004**, *108*, 5930.

(7) Wang, Y.-H.; Siu, W.-K. *Can. Geotech. J.* **2006**, *43*, 587.

(8) Hu, X. L; Michaelides, A. *Surf. Sci.* **2007**, *601*, 5378.

(9) Hu, X. L; Michaelides, A. *Surf. Sci.* **2008**, *602*, 960.

(10) Berendsen, H. J. C.; Grigera, J. R.; Straatsma, T. P. *J. Phys. Chem.* **1987**, *91*, 6269.

(11) Lisal, M.; Nezbeda, I.; Smith, W. R. *J. Phys. Chem. B* **2004**, *108*, 7412.

(12) Cygan, R. T.; Liang, J.-J.; Kalinichev, A. G. *J. Phys. Chem. B* **2004**, *108*, 1255.

(13) Vega, C.; Sanz, E.; Abascal, J. L. F. *J. Chem. Phys.* **2005**, *122*, 114507.

(14) Mahoney, M. W.; Jorgensen, W. L. *J. Chem. Phys.* **2000**, *112*, 8910.

(15) Bish, D. L. *Clays Clay Miner.* **1993**, *41*, 783.

(16) Shelley, J. C.; Patey, G. N. *Mol. Phys.* **1996**, *88*, 385.

(17) Yeh, I.-C.; Berkowitz, M. L. *J. Chem. Phys.* **1999**, *111*, 3155.

(18) Allen, M. P.; Tildesley, D. J. *Computer Simulation of Liquids*; Clarendon: Oxford, U.K., 1989.

(19) Delville, A. *J. Phys. Chem.* **1995**, *99*, 2033.

(20) Riemer, N.; Vogel, H.; Vogel, B.; Schell, B.; Ackermann, I.; Kessler, C.; Hass, H. *J. Geophys. Res.* **2003**, *108* (D4), 4144.

(21) Dentener, F. J.; Crutzen, P. J. *J. Geophys. Res.* **1993**, *98*, 7149.

(22) Turnbull, D.; Vonnegut, B. *Ind. Eng. Chem.* **1952**, *44*, 1292.

(23) Shevkunov, S. V. *Colloid. J.* **2005**, *67*, 497.

(24) Shevkunov, S. V. *Colloid. J.* **2007**, *69*, 360.

(25) Taylor, J. H.; Hale, B. N. *Phys. Rev. B* **1993**, *47*, 9732.

(26) Wassermann, B.; Reif, J.; Matthias, E. *Phys. Rev. B* **1994**, *50*, 2593.

(27) Cerdá, J.; Michaelides, A.; Bocquet, M.-L.; Feibleman, P. J.; Mitsui, T.; Rose, M.; Fomin, E.; Salmeron, M. *Phys. Rev. Lett.* **2004**, *93*, 116101–1.

(28) Michaelides, A.; Morgenstern, K. *Nat. Mater.* **2007**, *6*, 597.

JP805615Q